Supplement (Supporting Information) for

Leeuwin Current dynamics over the last 60 kyrs – relation to Australian extinction and Southern Ocean change

Dirk Nürnberg[1], Akintunde Kayode[1], Karl Meier[2], Cyrus Karas[3]

[1]GEOMAR Helmholtz Centre for Ocean Research Kiel, Wischhofstr. 1-3, D-24148 Kiel, Germany

[2]Institute of Earth Science, Heidelberg University, Im Neuenheimer Feld 234, Heidelberg D-69120, Germany

[3]Universidad de Santiago de Chile, Av. Bernardo O'Higgins 3363, Santiago, Chile

Correspondence to: Dirk Nürnberg (dnuernberg@geomar.de)

Introduction

The Supplement includes text passages, figures, and data tables supporting the abovementioned study. The text discusses in higher detail the ecology of the selected foraminiferal species, and diverse aspects relevant to the Mg/Ca-paleothermometry.

1. **Text S1** Supporting information on foraminiferal species selected and their ecology, analytical details and error assessment for foraminiferal Mg/Ca, contamination and calcite dissolution issues, and references.
2. **Figure S1.** Contamination plots (core 2614)
3. **Figure S2.** Contamination plots (core 2609)
4. **Figure S3.** Downcore Mg/Ca*O.universa* of core 2614
5. **Figure S4.** Downcore Mg/Ca*O.universa* of core 2609
6. **Figure S5.** Downcore Mg/Ca*G.trunca* of core 2609
7. **Figure S6.** Analytical results for western core 2614
8. **Figure S7.** Analytical results for eastern core 2609
9. **Figure S8.** Calculated Mg/Ca-based temperatures from western core 2614
10. **Figure S9.** Calculated Mg/Ca-based temperatures from eastern core 2609
11. **Table S1.** Defined outliers

Text S.1 Supporting information on foraminiferal species selected and their ecology, analytical details, and error assessment for foraminiferal Mg/Ca, contamination and calcite dissolution issues, and references.

Ecology, calcification depths, and seasonality of proxy formation

Planktonic foraminifera are marine protists living in the photic zone. They produce calcitic tests from calcium carbonate from the surrounding water. To reconstruct surface ocean conditions, we selected the near-surface species *Orbulina universa* (d'Orbigny, 1839). *O. universa* is a spinose planktonic foraminiferal species that inhabits surface waters throughout the tropical, subtropical and transition zones of the world ocean (Bé and Tolderlund, 1971). Early studies of their habitat preferences and morphology regard their morphotypes as belonging to the same genetic species, but showing phenotypic variations under different environmental conditions (Bé et al., 1973; Hecht et al., 1976; Colombo and Cita, 1980). These studies reveal that *O. universa* has a preference for dwelling within the photic zone between the surface mixed layer and the shallow thermocline, which is ~30-80 m water depth in our study areas (c.f. Fig. 2). *O. universa* has a 2-staged growth in their life cycle (Caron et al., 1987; Lea et al., 1995). In the juvenile stage, they build a multi-chambered trochospiral form covered with calcite spines. In the adult stage, they develop a final, large, spherical chamber that hosts 90-95% of its total calcite (Spero and Parker, 1985). The final chamber continues to thicken until gametogenesis, during which their spines are shed (Hamilton et al., 2008).

Based on sediment trap studies, Deuser et al. (1981) proposed different calcification depths for different morphotypes of *O. universa*: thin-walled (5-10 μm) and thick-walled (up to 30 μm) morphotypes, with the thick-walled morphotypes secreting shells having ~0.5‰ higher $\delta^{18}O$ than the thin-walled variants. Marshall et al. (2015) pointed out that the different isotopic compositions of both morphotypes cannot be explained by seasonal variation, as they are both present year-round. For this study, we made no distinction between morphotypes, as both morphotypes of *O. universa* show resembling calcification depths (Anand et al., 2003; Farmer et al., 2007). The issue of a seasonal bias of proxies generated on *O. universa* is discussed further below.

To support the *O. universa* analytical results, we additionally analyzed *Globigerinoides ruber* white, which is a symbiont-bearing near surface dwelling species, living in the upper 50 m of the mixed layer (Bé and Hutson, 1977). It occurs in warmer regions, predominantly in subtropical regions. Several studies confirmed that *G. ruber* records reflect warmest water

conditions of the seasonal cycle (Regenberg, et al., 2009). Andrijanic (1988) showed omnipresent *G. ruber* in austral summer off the eastern Australian coast. We presume that *G. ruber* did not change habitat significantly over time, as it is a very shallow dwelling, symbiont-bearing species dependent on high light levels.

To reconstruct subsurface ocean properties, we selected calcitic tests of the planktonic foraminiferal species *Globorotalia truncatulinoides* (d´Orbigny, 1839). *G. truncatulinoides* is a deep-dwelling planktonic, subtropical species, which occurs over a broad range of water temperatures and salinities (e.g., Lohmann and Schweitzer, 1990; Ganssen and Kroon, 2000). For *G. truncatulinoides,* a coiling dimorphism is apparent, separating the species into left-coiled (sinistral) and right-coiled (dextral) morphotypes. The preferred habitats of both morphotypes, however, are rather similar (Jentzen et al., 2018; Cléroux et al., 2008). Friedrich et al. (2012) and Ganssen and Kroon (2000) found that both morphotypes have similar stable oxygen ($\delta^{18}O$) and carbon isotope ($\delta^{13}C$) compositions, and Mg/Ca signatures. We therefore made no distinctions between morphotypes.

G. truncatulinoides exhibits a complex life cycle, beginning in the upper meters of the water column in the photic zone. It continues to grow and calcify new chambers in deeper waters until it reaches the adult stage, thereby pursuing a reproductive strategy that requires annual vertical migration of several hundred meters, with greater living depths during spring and summer (Cléroux et al., 2009). Different encrustation stages of *G. truncatulinoides*, in this respect, may point to different calcification depths (Reynolds et al., 2018). In the Gulf of Mexico, non-encrusted and encrusted specimens reveal mean calcification depths of 66 ± 9 m (with a range between 0-150 m) and 379 ± 76 m (with a range between 170 and 700 m), respectively (Reynolds et al., 2018). As the majority of the *G. truncatulinoides* specimens in cores 2614 and 2609 are encrusted, we assume a rather deep habitat depth range.

Various studies reported that a higher abundance of *G. truncatulinoides* is associated with a very deep (permanent) thermocline and/or thick water thermostads (Lohmann and Schweitzer, 1990; Ravelo and Fairbanks, 1992; McKenna and Prell, 2004; Schiebel and Hemleben, 2005). In Tobago basin (tropical W-Atlantic), Nürnberg et al. (2021) assigned a calcification depth of ~200-250 m to *G. truncatulinoides*, which corresponds to a depth nearly below the main thermocline in this area. This notion is in good agreement with findings from the eastern Caribbean, where *G. truncatulinoides* apparently prefers a habitat at ~180-300 m (Jentzen et al., 2018). Cléroux et al. (2008) proposed that at mid-latitudes and high latitudes, the isotopic temperature of *G. truncatulinoides* exceeds winter temperatures, but coincide with summer temperatures around the base of the summer thermocline. In our study area, the base of the

summer thermocline is between ~350 and 400 m (Fig. 2), which is rather deep compared to other ocean areas.

Jonkers and Kučera (2015) projected that the flux pattern of the deep-dwelling *G. truncatulinoides* is rather regular over the year, with a high percentage of the annual flux occurring in a single high-flux pulse. For our derived $subSST_{Mg/Ca}$ records we reckon that the seasonal range at the base of the thermocline is minimal (Fig. 2), hence a seasonal bias for the proxy records, if any, is minimal.

Sample contamination

Marine sediment contains a significant proportion of clay (~1-10 % Mg by weight), which may perturb the foraminifereal Mg/Ca ratios, when tests are not cautiously cleaned prior to the analyses. By monitoring the foraminiferal samples for their Fe/Ca, Al/Ca and Mn/Ca ratios, the effect of cleaning efficiency, post depositional contamination, and diagenetic alteration on foraminiferal Mg/Ca was examined. Barker et al. (2003) and Them et al. (2015) proposed contamination-indicative threshold values for Fe/Ca, Al/Ca and Mn/Ca (<0.1 mmol/mol). Meanwhile, numerous studies have shown that these threshold values - defined in the North Atlantic - are often exceeded as they largely depend on the sediment type the foraminiferal tests were removed from (e.g. Nünberg et al., 2015; 2021).

In many of our foraminiferal samples, the Al/Ca, Fe/Ca and Mn/Ca ratios are higher than the given threshold values, and at times reach values of up to ~0.7 mmol/mol, ~0.5 mmol/mol, and ~0.007 mmol/mol, respectively (Fig. S1; S2). Notably, these high contaminant values do not consistently have extremely high foraminiferal Mg/Ca ratios. Also, the correlation of $Mg/Ca_{O.universa}$ to either Al/Ca, Fe/Ca, or Mn/Ca for the core 2614 is insignificant (R^2= 0.0047, 0.0095 and 0.0497), suggesting that samples were not contaminated (Fig. S1). A high covariance between Mg/Ca and Mn/Ca, Fe/Ca and/or Al/Ca would imply insufficient clay removal during cleaning (Barker et al., 2003). Low correlation coefficients are also present in *O. universa* (R^2= 0.24, 0.32 and 0.14) and *G. truncatulinoides* samples from core 2609 (R^2= 0.62, 0.58 and 0.02) (Fig. S2).

In Figures S3–S5, the downcore comparison of Mg/Ca ratios to the contaminant element ratios Al/Ca, Fe/Ca and Mn/Ca are shown. From the comparisons, unusually high Mg/Ca ratios relative to contaminant element ratios were excluded from the downcore records, as they led to unrealistically high temperature estimates (Tab. S1).

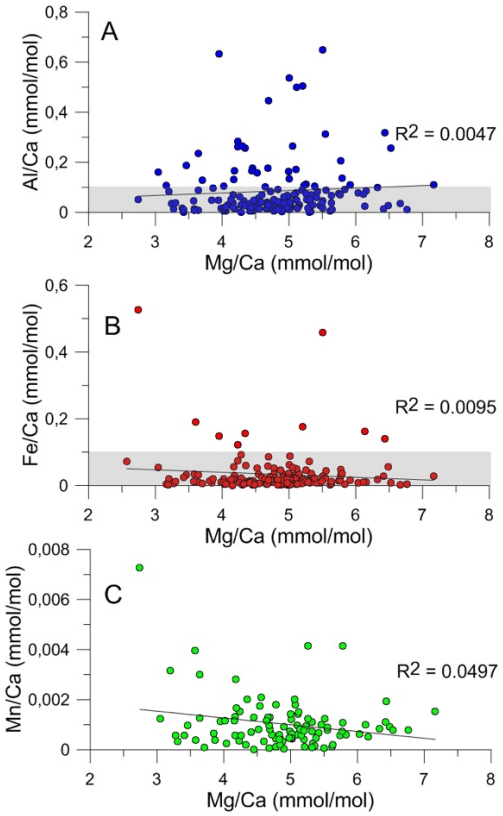

Figure S1. Contamination plots. Foraminiferal Mg/Ca vs. Al/Ca (blue), Fe/Ca (red) and Mn/Ca (green) for *O. universa* from core 2614. Al/Ca, Fe/Ca and Mn/Ca partly exceed threshold values (>0.1 mmol/mol, gray shading) proposed by Barker et al. (2003). R^2 = correlation coefficients.

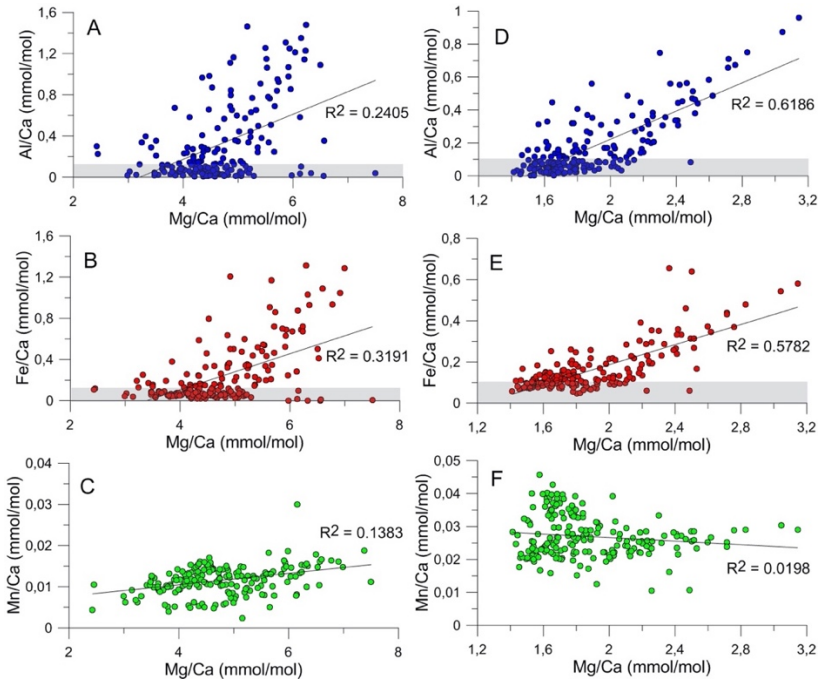

Figure S2. Contamination plots. Foraminiferal Mg/Ca vs. Al/Ca (blue), Fe/Ca (red) and Mn/Ca (green) for *O. universa* (left; A, B, C) and *G. truncatulinoides* (right; D, E, F) from core 2609. Al/Ca, Fe/Ca and Mn/Ca partly exceed threshold values (>0.1 mmol/mol, gray shading) proposed by Barker et al. (2003). R^2 = correlation coefficients.

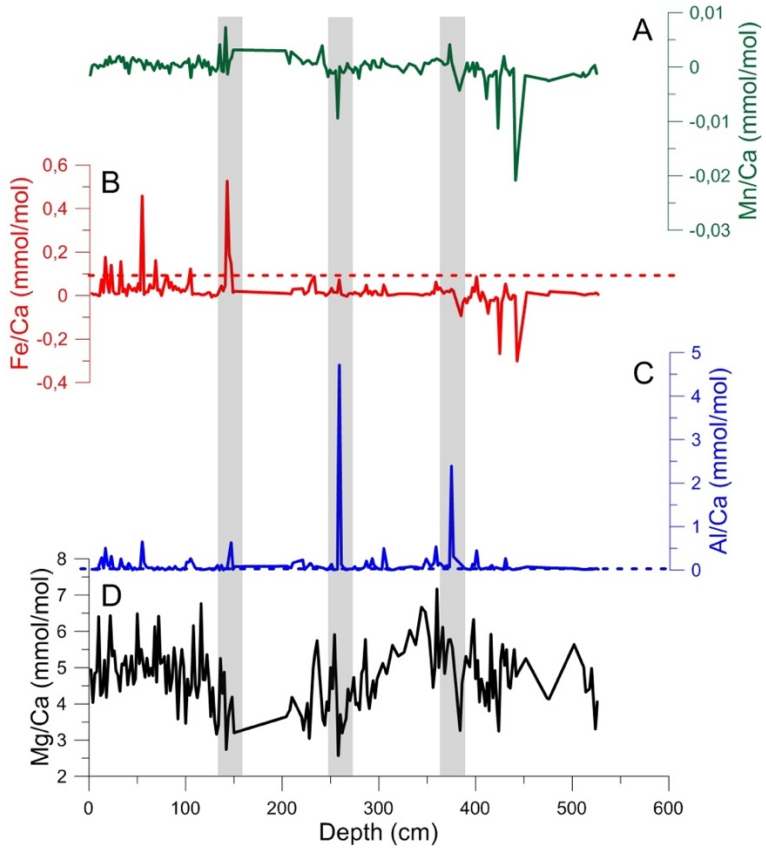

Figure S3. Downcore Mg/Ca$_{O.universa}$ of core 2614 (D) in comparison to contaminant elemental ratios Al/Ca (C), Fe/Ca (B), and Mn/Ca (A) from the same samples. Correlation coefficients are given in Fig. S1. Threshold values provided by Barker et al. (2003) indicative of sample contamination (>0.1 mmol/mol) are indicated by the dashed lines, but should be viewed cautiously. Gray shaded bars mark the excluded samples (c.f. Tab. S1).

Table S1. Defined outliers with unusually high contaminant ratios taken out from further interpretations.

Core	Sample depth (cm)	Sample species	Mg/Ca (mmol/mol)	Al/Ca (mmol/mol)	Fe/Ca (mmol/mol)	Mn/Ca (mmol/mol)
2614	142	*O. universa*	2.74	0.052	0.53	0.007
	258		2.57	4.72	0.072	-0.009
	374		5.78	2.39	0.03	0.004
		G. truncatulinoides	-	-	-	-
2609	64	*O. universa*	7.38	3.96	1.96	0.019
	166		4.92	2.22	1.21	0.08
	190		6.05	3.66	1.69	0.015
	26	*G. truncatulinoides*	2.46	0.56	0.46	0.03
	52		3.04	0.87	0.54	0.03
	96		3.14	0.96	0.58	0.03

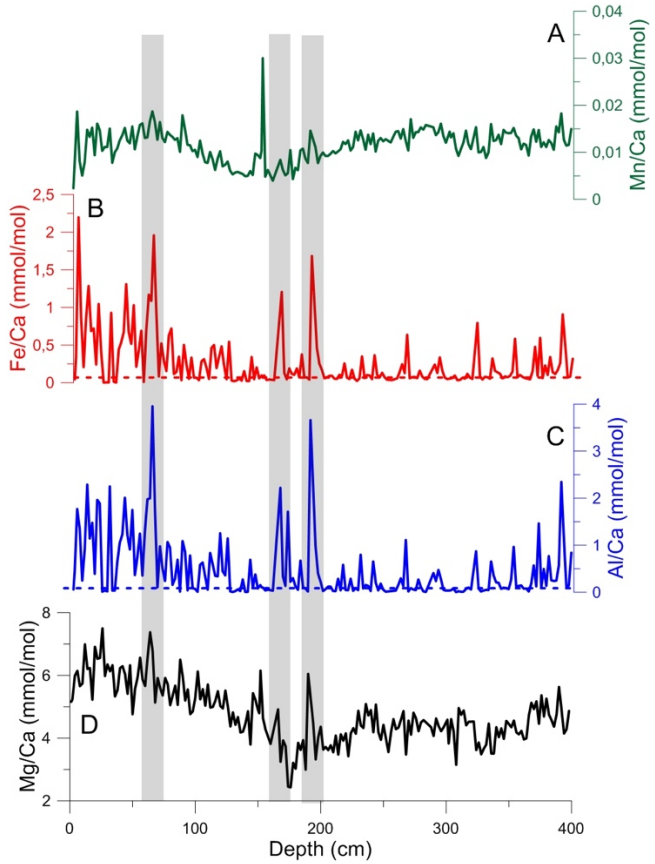

Figure S4. Downcore Mg/Ca*O.universa* of core 2609 (D) in comparison to contaminant elemental ratios Al/Ca (C), Fe/Ca (B), and Mn/Ca (A) from the same samples. Correlation coefficients are given in Fig. S2. Threshold values provided by Barker et al. (2003) indicative of sample contamination (>0.1 mmol/mol) are indicated by the dashed lines, but should be viewed cautiously. Gray shaded bars mark the excluded samples (c.f. Tab. S1).

Calcite dissolution effects and preferential Mg-ion removal

Calcite dissolution in fact lowers foraminiferal Mg/Ca-based temperature estimates (e.g., Nürnberg et al., 1996; Regenberg et al., 2006). Nonetheless, many studies prove the large potential of the Mg/Ca-paleothermometry even in calcite-unsaturated waters (e.g., Nürnberg et al., 2015; Tapia et al., 2015). Approaches were introduced to correct for the Mg^{2+}-ion loss, either by correcting for water depth (e.g., Regenberg et al., 2006; Dekens et al., 2002) or by correcting for the degree of undersaturation with respect to calcite ion concentration (e.g., Regenberg et al., 2006; 2014). In the study area, the calcite saturation state $\Delta([CO_3^{2-}])$, which is the difference between the *in situ* carbonate ion concentration ($[CO_3^{2-}]$) and ($[CO_3^{2-}]$) at saturation, is 0 µmol kg^{-1} at >3700 m water depth today (Regenberg et al., 2006). The ~21.3 ± 6.6 µmol kg^{-1} threshold being considered as critical for selective Mg^{2+}-removal (Regenberg et al., 2006; 2014) is clearly shallower at ~1500 m water depth in the study area. While our western core 2614 from a water depth of 1070 m is above this critical threshold level, the

eastern core 2609 is ~500 m below this threshold level, making the dissolution-related perturbation of the Mg/Ca-signal possible. Nonetheless, the Holocene mean $SST_{Mg/Ca}$ and $subSST_{Mg/Ca}$ estimates appear close to the modern temperatures at the respective water depths (Fig. 2) suggesting that selective Mg^{2+}-ion removal due to calcite dissolution processes is rather negligible.

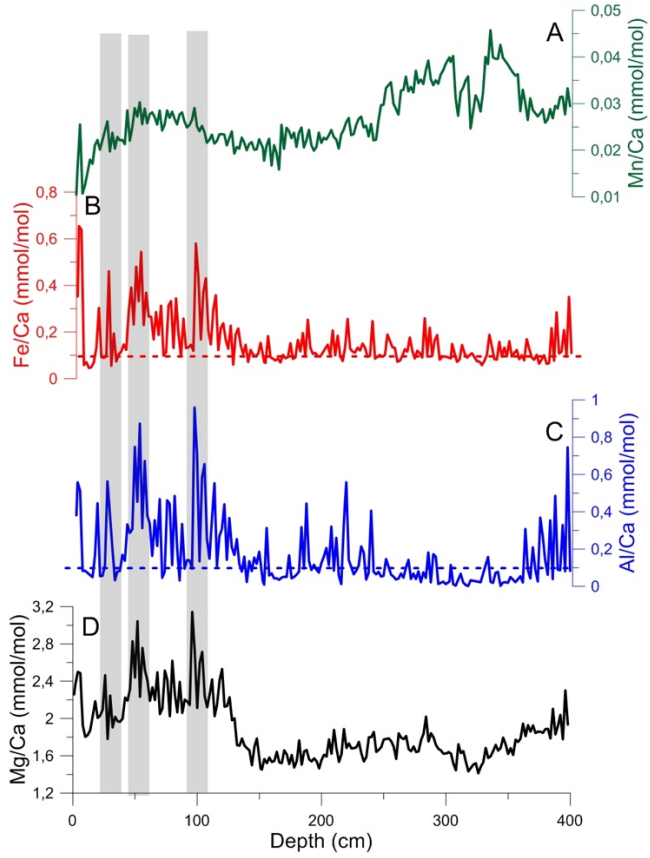

Figure S5. Downcore $Mg/Ca_{G.trunca}$ of core 2609 (D) in comparison to contaminant elemental ratios Al/Ca (C), Fe/Ca (B), and Mn/Ca (A) from the same samples. Correlation coefficients are given in Fig. S2. Threshold values provided by Barker et al. (2003) indicative of sample contamination (>0.1 mmol/mol) are indicated by the dashed lines, but should be viewed cautiously. Gray shaded bars mark the excluded samples (c.f. Tab. S1).

Analytical results: Oxygen isotopes ($\delta^{18}O$) and Mg/Ca ratios

Western core 2614

The $\delta^{18}O_{G.ruber}$ record of core 2614 (van der Kaars et al , 2017) is rather similar to the $\delta^{18}O_{O.universa}$ record with respect to downcore variations and the deglacial amplitude change, although absolute $\delta^{18}O_{G.ruber}$ values are on average higher by ~0.5‰. The $\delta^{18}O_{universa}$ record is generally lighter than the $\delta^{18}O_{G.trunca}$ record, with $\delta^{18}O_{O.universa}$ showing a range between 0.1 and 1.5‰, while $\delta^{18}O_{G.trunca}$ values are heavier ranging between 0.6 and 3.5‰ (Fig. S6). The species-specific $\delta^{18}O$-values hence, reflect the according living depths of the three species.

The downcore variations in $Mg/Ca_{universa}$ are broadly reflected by $Mg/Ca_{G.ruber}$, although the amplitude fluctuations appear to be larger in $Mg/Ca_{O.universa}$. $Mg/C_{O.universa}$ is overall higher (~3-7.5 mmol/mol) than $Mg/Ca_{G.trunca}$, (~0.8-5.2 mmol/mol) (Fig. S6). Notably, $Mg/Ca_{G.trunca}$ exhibits various prominent excursions to extremely high values >4.5 mmol/mol and amplitudes of >4 mmol/mol.

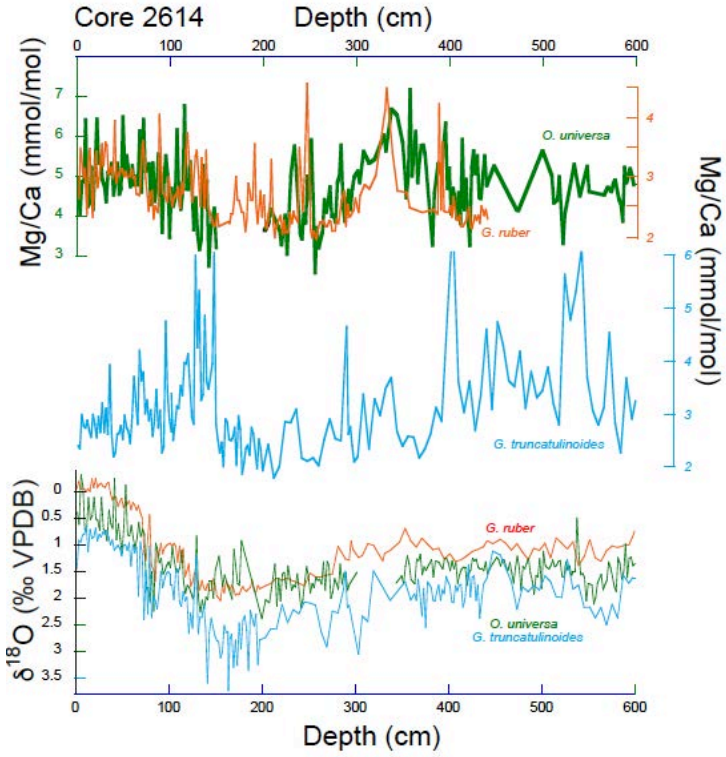

Figure S6. Analytical results for western core 2614. Top: Mg/Ca ratios of *G. ruber* (orange), *O. universa* (green) and *G. truncatulinoides* (light blue). Bottom: Species-specific $\delta^{18}O$ records. The $\delta^{18}O_{G.ruber}$ data are from van der Kaars et al. (2017).

Eastern core 2609

Similar to core 2614, the absolute $\delta^{18}O$ values in the eastern core 2609 reflect the increasing calcification depths of the studied species, with $\delta^{18}O_{G.trunca} > \delta^{18}O_{O.universa} > \delta^{18}O_{G.ruber}$. The $\delta^{18}O_{G.ruber}$ record is lighter by on average ~0.5‰ than the $\delta^{18}O_{O.universa}$ record, while their downcore amplitude variations are quite similar (Fig. 7). Both records are lighter by ~0.7-2‰ than the $\delta^{18}O_{G.trunca}$ record. Notably, the downcore $\delta^{18}O_{G.trunca}$ variations are larger than those of the surface-dweller. They resemble those of core 2614, but are clearly heavier (Fig. S6).

The $Mg/Ca_{universa}$ and $Mg/Ca_{G.trunca}$ records range between ~3-5-7 mmol/mol, and downcore variations are rather similar not exceeding ~2 mmol/mol (Fig. S7). The $Mg/Ca_{G.trunca}$ record is on average ~4 mmol/mol lower than those of the shallow-dweller, and exhibits significantly

lowered $Mg/Ca_{G.trunca}$ below ~1.4 m core depth. Compared to core 2614, the core 2609 $Mg/Ca_{G.trunca}$ record shows only small-scale amplitude variations of >1 mmol/mol.

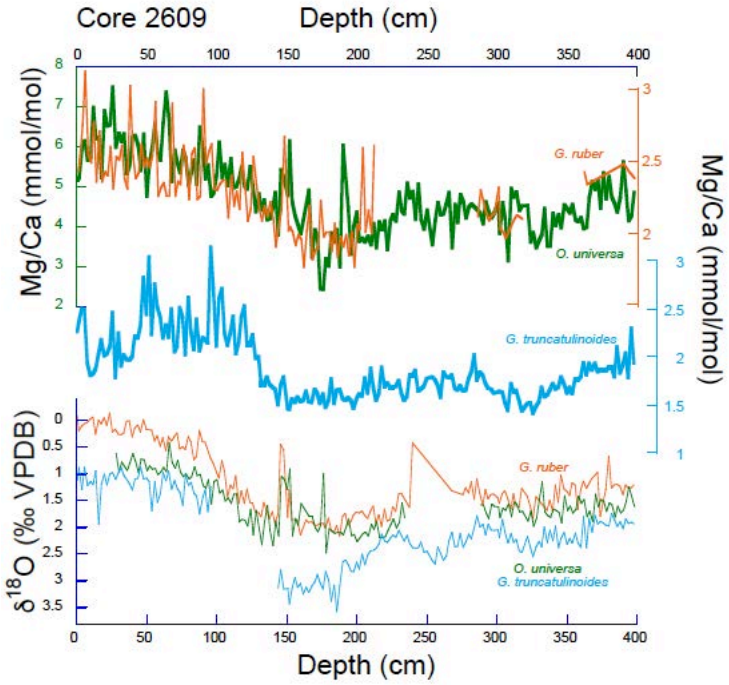

Figure S7. Analytical results for eastern core 2609. Top: Mg/Ca ratios of *G. ruber* (orange), *O. universa* (green) and *G. truncatulinoides* (light blue). Bottom: Species-specific $\delta^{18}O$ records.

Foraminiferal Mg/Ca-paleothermometry

O. universa

The Mg/Ca ratios of *O. universa* were converted into sea surface temperatures ($SST_{Mg/Ca}$) using available species-specific temperature calibrations (c.f. Fig. S8, S9). We finally chose the calibration equation of Hathorne et al. (2003). This calibration function (Mg/Ca = 0.95 exp(0.086 SST)) is based on *O. universa* specimens recovered from a latitudinal transect in the North Atlantic to monitor their Mg-uptake. Compared to the Lea et al. (1999), Anand et al. (2003a), Russell et al. (2004), and Regenberg et al. (2009) equations (Mg/Ca = 1.36 exp(0.085 SST); Mg/Ca = 0.38 exp(0.09 SST); Mg/Ca = 0.85 exp(0.096 SST); Mg/Ca = 0.29 exp(0.101 SST)), the calibration of Hathorne et al. (2003) provides core-top (late Holocene) $SST_{Mg/Ca}$, which are in broad agreement with the modern austral summer SST ranges at ~30-80 m water depth in the upper thermocline/mixed layer (Fig. S8, S9).

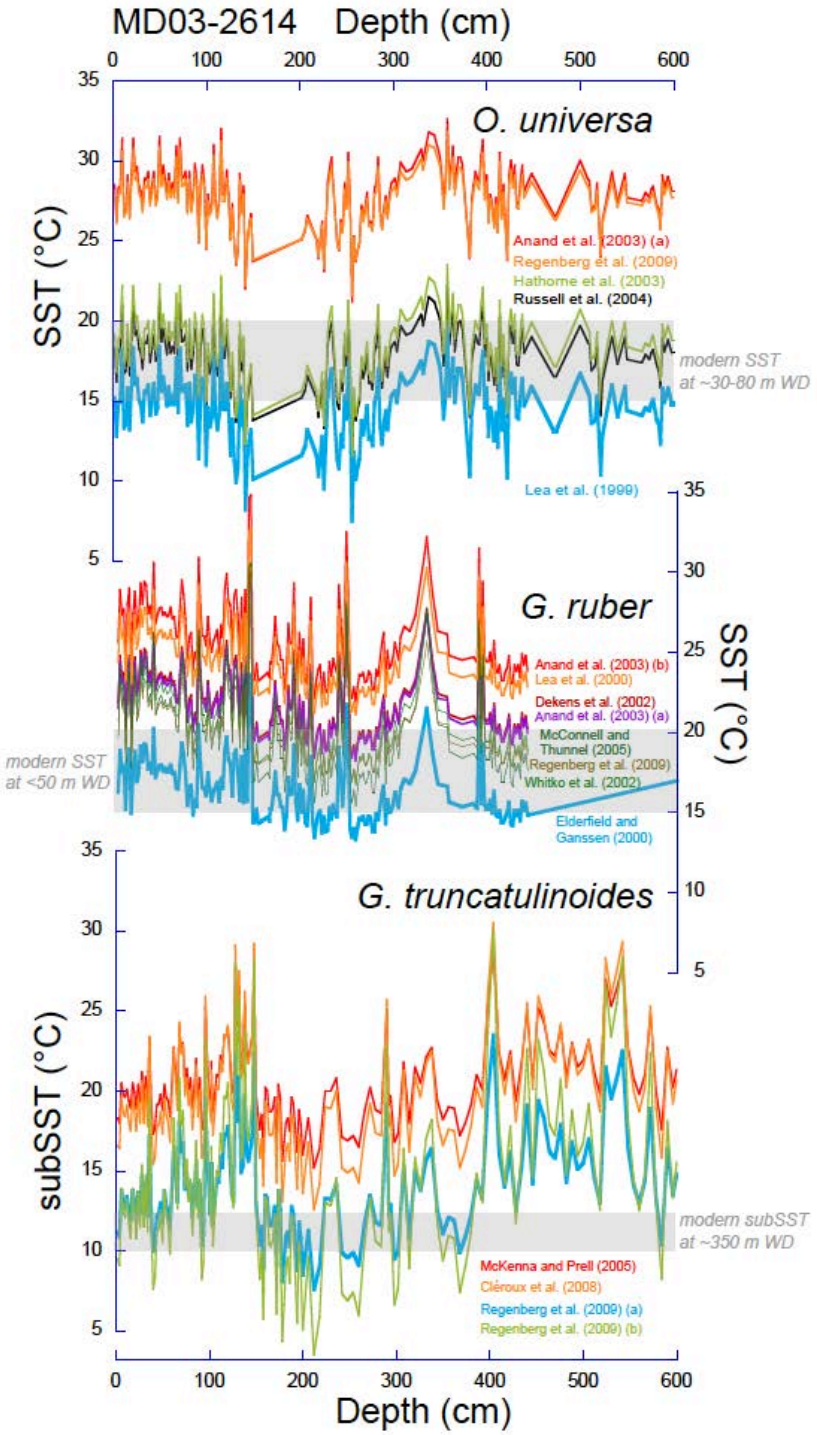

Figure S8. Calculated Mg/Ca-based temperatures from 0-600 cm core depth for western core 2614. The Mg/Ca data of *O. universa*, *G. ruber*, and *G. truncatulinoides* were converted using species-specific temperature calibrations (c.f. legend). Modern annual SST at ~30-80 m, <50 and ~350 mwd are indicated (WOA, Locarnini et al., 2018), which are the most likely habitats of the studied species.

G. ruber

Although the Mg/Ca ratios of *G. ruber* follow in course and amplitude the according records of *O. universa*, and can be therefore taken as reliable support, we refrained from calculating

234 $SST_{Mg/Ca}$ from Mg/Ca_{ruber} due to the following reasons: All temperature equations available for
235 *G. ruber* (Lea et al., 2000: Mg/Ca = 0.30 exp (0.089 SST); Anand et al., 2003: Mg/Ca =
236 0.38 exp(0.09 SST), Mg/Ca = 0.342 exp(0.09 SST); Dekens et al., 2002: Mg/Ca =
237 0.37 exp(0.09(SST-0.36(core depth in km)-2.0°C); McConell and Thunnel et al., 2005: Mg/Ca
238 = 0.69 exp(0.068 SST); Regenberg et al., 2009: Mg/Ca = 1.43 exp(0.047 SST); Whitko et al.,
239 2002: Mg/Ca = 0.57 exp(0.074 SST)) provide SSTs, which are warmer by several degrees than
240 the modern austral summer SST at <50 m water depth, and reach unrealistic paleo-SST of even
241 >30°C in the western core 2614 (Fig. S8, S9). Only the Elderfield and Ganssen (2000) equation
242 (Mg/Ca = 0.52 exp (0.10SST)) provides a late Holocene $SST_{Mg/Ca}$, which comes close to the
243 modern austral summer SST at <50 m water depth (15-16°C at core location 2609; 17-19°C at
244 core location 2614). The core-top $SST_{Mg/Ca}$-estimates derived from *G. ruber* are hence, quasi
245 equally warm than those of *O universa*. As the Elderfield and Ganssen (2000) equation,
246 however, is a non-species-specific calibration but relies on various planktonic foraminiferal
247 species, we assess this equation not applicable and hence, do not use the *G. ruber* proxy data
248 for further interpretation.
249
250 *G. truncatulinoides*
251 The Mg/Ca ratios of the deep-dwelling *G. truncatulinoides* were converted into subsurface
252 temperatures ($subSST_{Mg/Ca}$) using the calibration equation of Regenberg et al. (2009) (Mg/Ca
253 = 1.32 exp(0.05 TT)). The Regenberg et al. (2009) study was based on calibrating Mg/Ca ratios
254 of multiple planktonic foraminifera species (including *G. truncatulinoides*) obtained from
255 (sub)tropical Atlantic sediment-surface samples with $\delta^{18}O$-derived calcification temperatures.
256 The calibration provided Holocene $subSST_{Mg/Ca}$ estimates, which agree with the modern annual
257 thermocline temperatures at the preferred depth of *G. truncatulinoides* in our study area (Fig.
258 S8, S9). The error (standard deviation 2σ) is ±1.0°C. Other existing paleotemperature
259 calibrations specific to *G. truncatulinoides* (e.g., McKenna and Prell, 2005: Mg/Ca =
260 0.355 exp(0.098 TT); Cléroux et al., 2008: Mg/Ca = 0.62 exp(0.074 TT); Regenberg et al.,
261 2009: Mg/Ca = 0.84 exp (0.083 TT) and Mg/Ca = 1.32 exp (0.05 TT)) provide $TT_{Mg/Ca}$
262 estimates that are >7°C warmer than modern annual subsurface temperatures.
263 Growth seasonality is a relevant factor, which influences planktonic foraminiferal proxies and
264 creates seasonal biases in the proxy signal recorded in a fossil assemblage (Jonkers and Kučera,
265 2015). The Holocene $SST_{Mg/Ca}$ estimates from the eastern core region are ~3-5°C warmer than
266 the modern annual temperature range in the region. We take this as indication that the derived
267 $SST_{Mg/Ca}$ values represent the austral summer range during the Holocene. A seasonal bias for

the reconstructed $TT_{Mg/Ca}$ records is considered minimal, although Jonkers and Kučera (2015) noted that the flux pattern of *G. truncatulinoides* is focused towards winter and spring. Overall, we presuppose that the habitat depths of the selected planktonic foraminifera are relatively stable through time.

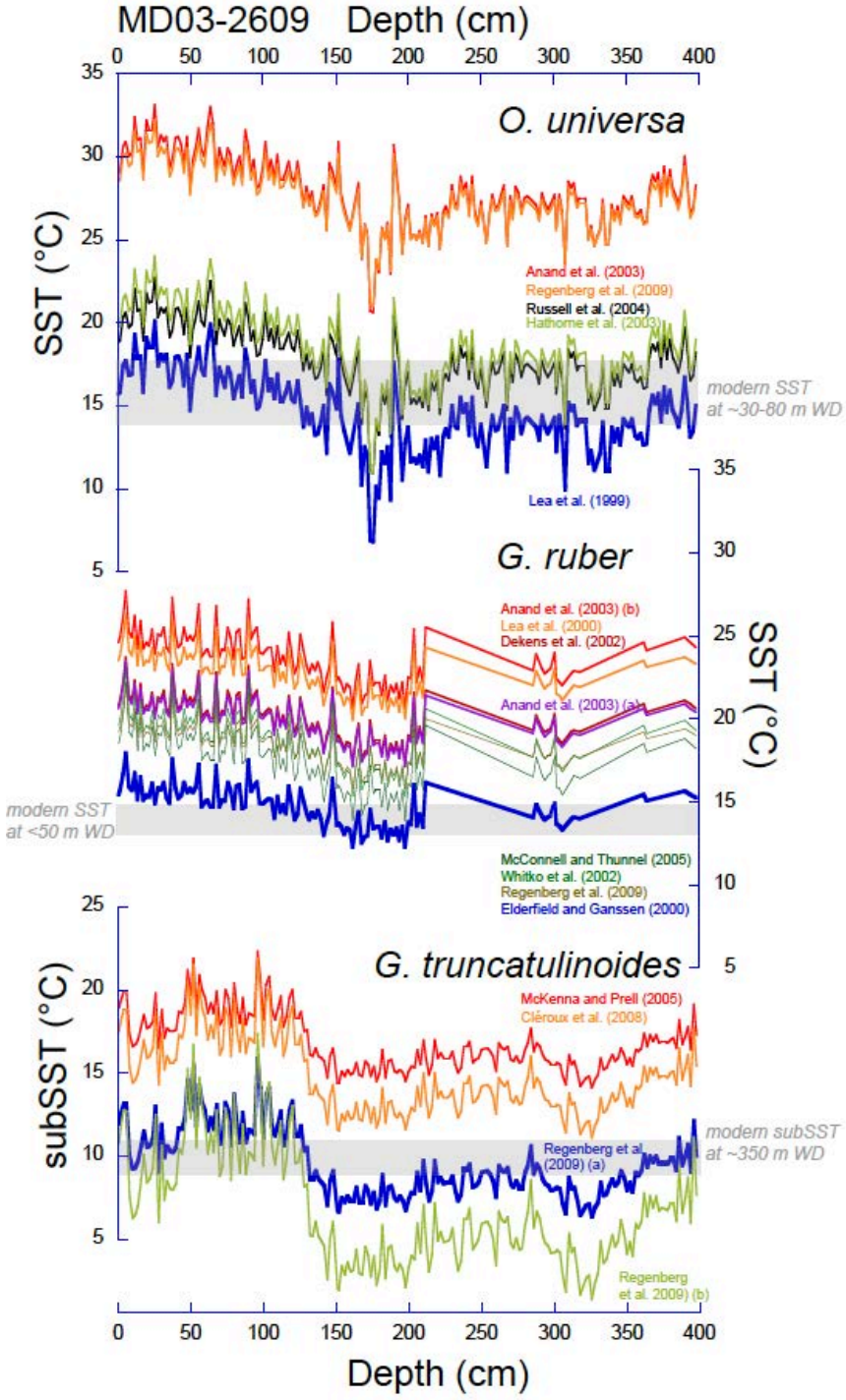

Figure S9. Calculated Mg/Ca-based temperatures from 0-400 cm core depth for eastern core 2609. The Mg/Ca data of *O. universa*, *G. ruber* and *G. truncatulinoides* were converted using species-specific temperature calibrations (c.f. legend). Modern annual SST at ~30-80 m, <50 and ~350 mwd are indicated (WOA, Locarnini et al., 2018), which are the most likely habitats of the studied species.

References

Andrijanic, S. (1988). Geographical distribution of living planktonic foraminifera (Protozoa) off the east coast of Australia. *Marine and Freshwater Research*, 39 (1), 71–85.

Anand, P., Elderfield, H., Conte, M.H. (2003). Calibration of Mg/Ca thermometry in planktonic foraminifera from a sediment trap time series. *Paleoceanography,* 18 (2).

Barker, S., Greaves, M., Elderfield, H. (2003). A study of cleaning procedures used for foraminiferal Mg/Ca paleothermometry. *Geochemistry, Geophysics, Geosystems*, 4(9), 8407, doi:10.1029/2003GC000559.

Bé, A.W.H., Tolderlund, D.S. (1971). Distribution and ecology of living planktonic foraminifera in surface water of the Atlantic and Indian Oceans. *Micropaleontology of Oceans,* Cambridge University Press, London, 105-149.

Bé, A.W.H., Hutson, W.H. (1977). Ecology of planktonic foraminifera and biogeographic patterns of life and fossil assemblages in the Indian Ocean. *Micropaleontology*, 23, 369-414.

Bé, A.W.H., Harrison, S.M., Lott, L. (1973). *Orbulina universa* d'Orbigny in the Indian Ocean. *Micropaleontology,* 19, 150-192.

Caron, D.A.W., Faber, W., Bé, A.W.H. (1987). Growth of the spinose planktonic foraminifer *Orbulina universa* in laboratory culture and the effect of temperature on life processes. *Journal of the Marine Biological Association of the United Kingdom*, 67 (2), 343-358.

Cléroux, C., Cortijo, E., Anand, P., Labeyrie, L., Bassinot, F., Caillon, N., Duplessy, J.-C. (2008). Mg/Ca and Sr/Ca ratios in planktonic foraminifera: Proxies for upper water column temperature reconstruction. *Paleoceanography,* 23 (3).

Cléroux, C., Lynch-Stieglitz, J., Schmidt, M.W., Cortijo, E., Duplessy, J.-C. (2009). Evidence for calcification depth change of *Globorotalia truncatulinoides* between deglaciation and Holocene in the western Atlantic Ocean. *Marine Micropaleontology*, 73, 57-61.

Colombo, M.R., Cita, M.B. (1980). Changes in size and test porosity of *Orbulina universa* d'Orbigny in the Pleisocene record of Cape Bojador (DSDP Site 397, eastern North Atlantic). *Marine Micropaleontology,* 5, 13-29.

Dekens, P.S., Lea, D.W., Pak, D.K., Spero, H.J. (2002). Core top calibration of Mg/Ca in tropical foraminifera: Refining paleotemperature estimation. *Geochemistry, Geophysics, Geosystems*, 3(4), 10.1029/2001GC000200.

Deuser, W.G., Ross, E.H., Hemleben, C., Spindler, M. (1981). Seasonal changes in species composition, numbers, mass, size and isotopic composition of planktonic foraminifera settling into the deep Sargasso Sea. *Paleoceanography. Paleoclimatology. Paleoecology* 33, 103-127.

Elderfield, H., Ganssen, G. (2000). Past temperature and delta18O of surface ocean waters inferred from foraminiferal Mg/Ca ratios. *Nature,* 405 (6785), 442-445.

Farmer, E.C., Kaplan, A., de Menocal, P.B., Lynch-Stieglitz, J. (2007). Corroborating ecological depth preferences of planktonic foraminifera in the tropical Atlantic with stable oxygen isotope ratios of core-top specimens. *Paleoceanography,* 22, 1-14.

Friedrich, O., Schiebel, R., Wilson, P.A., Weldeab, S., Beer, C.J., Cooper, M.J., Fiebig, J. (2012). Influence of test size, water depth and ecology on Mg/Ca, Sr/Ca, $\delta^{18}O$ and $\delta^{13}C$ in nine modern species of planktic foraminifers. *Earth and Planetary Science Letters,* 319-320, 133-145.

316 Ganssen, G., Kroon, D. (2000). The isotopic signature of planktonic foraminifera from NE Atlantic surface
317 sediments: Implications for the reconstruction of past oceanic conditions. *Journal of the Geological Society*,
318 157, 693-699.
319 Hamilton, C.P., Spero, H.J., Bijma, J., Lea, D.W. (2008). Geochemical investigation of gametogenetic calcite
320 addition in the planktonic foraminifera *Orbulina universa***.** *Marine Micropaleontology,* 68 (3), 256-267.
321 Hathorne, E.C., Alard, O., James, R.H., Rogers, N.W. (2003). Determination of intratest variability of trace
322 elements in foraminifera by laser ablation inductively coupled plasma-mass spectrometry. *Geochemistry,*
323 *Geophysics, Geosystems,* 4(12), 8408, doi:10.1029/2003GC000539.
324 Hecht, A.D., Bé, A.W.H., Lott, L. (1976). Ecologic and paleoclimatic implications of morphologic variation of
325 *Orbulina universa* in the Indian Ocean. *Science,* 194, 422-424.
326 Jentzen, A., Nürnberg, D., Hathorne, E.C., Schönfeld, J. (2018). Mg/ Ca and $\delta^{18}O$ in living planktic foraminifers
327 from the Caribbean, Gulf of Mexico and Florida Straits. *Biogeosciences*, 15 (23), 7077–7095.
328 https://doi.org/10.5194/bg-15-7077-2018.
329 Jonkers, L., Kucera, M. (2015). Global analysis of seasonality in the shell flux of extant planktonic foraminifera.
330 *Biogeosciences,* 12 (7), 2207-2226.
331 Lea, D.W., Martin, P.A., Chan, D.A., Spero, H.J. (1995). Calcium uptake and calcification rate in the planktonic
332 foraminifer *Orbulina universa*. *Journal of Foraminifera Research*, 25, 185-206.
333 Lea, D.W., Mashiotta, T.A., Spero, H.J. (1999). Controls on magnesium and strontium uptake in planktonic
334 foraminifera determined by live culturing. *Geochimica et Cosmochimica Acta* 63 (16), 2369-2379.
335 Lea, D.W., Pak, D.K., Spero, H.J. (2000). Climate impact of Late Quaternary equatorial Pacific sea surface
336 temperature variations. *Science,* 289, 1719-1724.
337 Locarnini, R.A., Mishonov, A.V., Baranova, O.K., Boyer, T.P., Zweng, M.M., Garcia, H.E., Reagan, J.R., Seidov,
338 D., Weathers, K.W., Paver, C.R., Smolyar, I.V. (2018). Temperature. NOAA Atlas NESDIS. In: Levitus, S.
339 (Ed.), World Ocean Atlas 2018 (1).
340 Lohmann, G.P., Schweitzer, P.N. (1990). *Globorotalia truncatulinoides'* growth and chemistry as probes of the
341 past thermocline: 1. Shell size. *Journal of Paleoceanography and Paloclimatology*.
342 https://doi.org/10.1029/PA005i001p0005.
343 Marshall, B.J., Thunell, R.C., Spero, H.J., Henehan, M.J., Lorenzoni, L., Astor, Y. (2015). Morphometric and
344 stable isotopic differentiation of *Orbulina universa* morphotypes from the Cariaco Basin, Venezuela. *Marine*
345 *Micropaleontology*, 10.1016/j.marmicro.2015.08.001.
346 McConnell, M.C., Thunell, R.C. (2005). Calibration of the planktonic foraminiferal Mg/Ca paleothermometer:
347 Sediment trap results from the Guaymas Basin, Gulf of California. *Paleoceanography*, 20, PA2016,
348 doi:10.1029/2004PA001077.
349 McKenna, V.S., Prell, W.L. (2004). Calibration of the Mg/Ca of *Globorotalia truncatulinoides* (R) for the
350 reconstruction of marine temperature gradients. *Paleoceanogrphy,* 19 (2).
351 https://doi.org/10.1029/2000PA000604.
352 Nürnberg, D., Bijma, J., Hemleben, C. (1996). Assessing the reliability of magnesium in foraminiferal calcite as
353 a proxy for water mass temperatures. *Geochimica et Cosmochimica Acta,* 60 (5), 803-814.
354 Nürnberg, D., Böschen, T., Doering, K., Mollier-Vogel, E., Raddatz, J., Schneider, R. (2015). Sea surface and
355 subsurface circulation dynamics off equatorial Peru during the last ~17 kyr. *Paleoceanography*, 30(7), 984–999.

Nürnberg, D., Riff, T., Bahr, A., Karas, C., Meier, K. Lippold, J. (2021). Western boundary current in relation to Atlantic Subtropical Gyre dynamics during abrupt glacial climate fluctuations. *Global and Planetary Change*, 201. doi: 10.1016/j.gloplacha.2021.103497.

Ravelo, A.C., Fairbanks, R.G. (1992). Oxygen isotopic composition of multiple species of planktonic foraminifera: Recorders of the modern photic zone temperature gradient. *Paleoceanography,* 7, 815-831.

Regenberg, M., Nürnberg, D., Steph, S., Groeneveld, J., Garbe-Schönberg, D., Tiedemann, R., Dullo, W.C. (2006). Assessing the effect of dissolution on planktonic foraminiferal Mg/Ca ratios: Evidence from Caribbean core tops. *Geochemistry, Geophysics, Geosystems,* 7(7), Q07P15. doi:10.1029/2005GC001019.

Regenberg, M., S. Steph, D. Nürnberg, R. Tiedemann, Garbe-Schönberg, D. (2009). Calibrating Mg/Ca ratios of multiple planktonic foraminiferal species with δ^{18}O-calcification temperatures: Paleothermometry for the upper water column. *Earth and Planetary Science Letters*, *278*(3), 324-336.

Regenberg, M., Regenberg, A., Garbe-Schönberg, D., Lea, D.W. (2014). Global dissolution effects on planktonic foraminiferal Mg/Ca ratios controlled by the calcite-saturation state of bottom waters. *Paleoceanography,* 29 (3), 127–142.

Reimer, P.J., Bard, E., Bayliss, A., et al. (2013). IntCal13 and Marine13 radiocarbon age calibration curves 0–50,000 years cal BP. *Radiocarbon,* 55 (4), 1869–1887.

Reynolds, C.E, Richey, J.N., Fehrenbacher, J.S., Rosenheim, B.E., Spero, H.J. (2018) Environmental controls on the geochemistry of *Globorotalia truncatulinoides* in the Gulf of Mexico: Implications for paleoceanographic reconstructions. *Marine Micropaleontology*, 142, 92–104. https://doi.org/10.1016/j.marmicro.2018.05.006.

Russell, A.D., Hönisch, B., Spero, H.J., Lea, D.L. (2004). Effects of seawater carbonate ion concentration and temperature on shell U, Mg, and Sr in cultured planktonic foraminifera. *Geochimica et Cosmochimica Acta*, 68 (21), 4347–4361. doi:10.1016/j.gca.2004.03.013.

Schiebel, R., Hemleben, Ch. (2005). Modern planktic foraminifera. *Paläontologische Zeitschrift*, 79 (1), 135–148.

Spero, H.J., Parker, S.L. (1985). Photosynthesis in the symbiotic planktonic foraminifera *Orbulina universa*, and its potential contribution to oceanic primary productivity. *Journal of Foraminifera Research,* 15, (4), 273-281.

Tapia, R., Nürnberg, D., Ronge, T., Tiedemann, R. (2015). Disparities in glacial advection of Southern Ocean Intermediate Water to the South Pacific Gyre. *Earth and Planetary Science Letters*, 410, 152–164. http://dx.doi.org/10.1016/j.epsl.2014.11.031.

Them, T.R., Schmidt, M.W., Lynch-Stieglitz, J. (2015). Millennial-scale tropical atmospheric and Atlantic Ocean circulation change from the last Glacial Maximum and Marine Isotope Stage 3. Earth and Planetary Science Letters, 427, 47–56.

Whitko, N., Hastings, D.W., Flower, B.P. (2002). Past sea surface temperatures in the tropical South China Sea based on a new foraminiferal Mg calibration. doi:MARSci.2002.01.020101.

van der Kaars, S., Miller, G.H., Turney, C.S.M., Cook, J.E., Nürnberg, D., Schönfeld, J., Kershaw, A.P., Lehman, S.J. (2017). Human rather than climate the primary cause of Pleistocene megafaunal extinction in Australia. *Nature Communications,* 8, 14142 https://doi.org/10.1038/ncomms14142.